INFORMATION REDACTED PURSUANT TOTHE FREEDOM
OF INFORMATION ACT (FOIA), 5 U.S.C.552(B)(6)

AES 12058074-5-1
May 2012

Failure Analysis of the Spring of a Haldex Spring Brake Chamber

Prepared By

Benjamin K. Jackson, Ph.D.

Intertek APTECH

Prepared For

Department of Transportation
Vehicle Research and Test Center
PO Box B-37
10820 SR 347
East Liberty, OH 43319-0337

Attention: Mr. Daniel G. Pearse
Email: dan.pearse@nhtsa.dot.gov

This report was prepared by Intertek APTECH as an account of work sponsored by the organization named herein. Neither Intertek APTECH nor any person acting on behalf of Intertek APTECH: (a) makes any warranty, express or implied, with respect to the use of any information, apparatus, method, or process disclosed in this report or that such use may not infringe privately owned rights; or (b) assumes any liabilities with respect to the use of, or for damages resulting from the use of, any information, apparatus, method, or process disclosed in this report.

FAILURE ANALYSIS OF THE SPRING OF A HALDEX SPRING BRAKE CHAMBER

BACKGROUND

Intertek APTECH was asked by the U. S. Department of Transportation Vehicle Research and Test Center (VRTC) to perform an independent failure analysis to determine the root cause of failures in polymer coated power springs in Haldex spring brake chambers (PN HDX1372430211). The chambers are used on heavy construction equipment and trucks to actuate the parking brake. The Office of Defect Investigation had received complaints of premature in-service failures of Haldex spring brake chambers, which resulted in at least one vehicle fire.

This is an ongoing investigation by the VRTC. The following data collected during the course of the investigation was provided to Intertek APTECH to aid in the investigation:

- A data table showing the testing that the VRTC had performed in their lab since receiving the brake chambers – images and data.
- Cassens Transport maintenance records showing the actual vehicle maintenance history for each of the chambers.
- Images of the spring brake chamber in operation, its disassembly, and images of fractures surfaces and debris found during initial testing in the VRTC lab.
- Data sheets showing the measured polymer coating thickness on each sample provided.
- Data showing the compositional analysis on debris found in each chamber after disassembly in the VRTC lab.
- Haldex promotional material documenting improvements to a superior line of Haldex brake chambers that are sealed from the environment. The document was helpful to

visualize the operation of the non-sealed chambers that were the subject of this investigation.

- A copy of a VRTC report on a chamber tested earlier for this investigation was provided. This report includes significant background detail on the operation of the chamber. This information is not included in this report to avoid duplication.
- Specifications used by Neway Anchorlok International, Inc. (NAI) for the acceptance of the spring wire, cold forming of the wire into springs, heat treatment, mechanical properties, dimensional requirements, and coating requirements. Springs produced under this specification to the dimensions specified by Haldex are those used in the spring brake chambers under investigation.

The following samples were provided to Intertek APTECH for analysis:

- One complete power spring that had not failed, but had been in service.
- Failed sections from four power springs. This included the two mating fracture surfaces and a small section from elsewhere in the spring coil (designated as 76039, 76369, 78023, and 78063).
- A section from a new spring that had not seen service (designated as LS-1).
- Two to three mounted and polished cross-sections were provided for each of the power spring samples.

VISUAL EXAMINATION

Images of the as-received samples are shown in Figures 1 through 3. The fractured power spring sections are shown in Figure 1, and Figures 2 and 3 show images of the intact spring.

Initial observations of the samples are as follows:

- The polymer coating (referred to as simply “paint” hereon) is only present in patches on the surfaces of the segments provided. The metal exposed where the paint is not present appears oxidized.
- The fracture surfaces are oxidized, but otherwise reasonably preserved.
- All failed samples with the exception of Sample 78063 showed a single fracture. Sample 78063 displayed a similar primary fracture with additional cracking.
- Figure 2 (a) shows the intact spring that was supplied. It did not display any visible cracking, but wear was evident on the spring surfaces in the form of patches of missing paint. Figure 2 (b) highlights the areas of missing paint showing exposed and oxidized metal beneath. The coils were numbered for ease of identification. Main areas of paint removal appear to be on Coils 1, 2, 4, and 5. These were the areas in contact with the housing end wall and pressure plate of the brake chamber. From the drawings and pictures supplied, it is apparent that the ends of the spring were simply positioned between the housing end wall and pressure plate and compressed approximately 50% of the free standing height. No lateral constraints were present.

SPRING COMPRESSION TEST

To ascertain the cause of the wear patterns observed on the intact spring, the spring was compressed using a Materials Test System (MTS). The results may be seen in Figure 3. The test was also captured on video and these files are supplied on the data DVD accompanying this report.

The spring was loaded into the MTS, and a polycarbonate safety shield placed around it. The ram of the machine was slowly raised on hydraulic pressure to compress the spring. The displacement of the ram was measured. The NAI specification (Section 4.2.1.2 of NS-65-99) specified that "the spring stroke shall be 1.5” to 4.0” total height." Since this is the section in which the functionality of the spring is to be tested for service, it is implied that this stroke is the intended operational range of the spring. The spring supplied had a free length (not

compressed) of 7.85 inches. During this test, the spring was compressed first by 3.0 inches to a total height of 4.85 inches (close to min-compression) and then by 4.5 inches to a total height of 3.35 inches (maximum travel of the ram, but within design compression range). The following observations were made:

- Figure 3 (a) shows the spring compressed by 3.0 inches. It is clear from the image that Coil 1 and Coils 4 and 5 are in contact with the ram/load cell. This is equivalent to the loading of the spring between the housing end wall and pressure plate in the spring brake chamber. The wear patterns on the spring shown in Figure 3 show a loss of paint in the regions where Coils 1, 4, and 5 contact the spring supports as in Figure 3 (a).

- When the spring is compressed further, Coil 2 contacts the spring support. Coils 3 and 4 do not quite touch at 4.5 inches compression (total height of 3.35 inches), but it is evident from the wear pattern observed that they did make contact during service, as is shown in Figure 3 (b) and (c). The MTS reached maximum travel at 4.5 inches, so it was not possible to demonstrate this in the test. Therefore, if it is to be believed that the stroke of 1.5 inches to 4.0 inches total height called out in Section 4.2.1.2 of NAI NS-65-99 is representative of normal operation, then the results of this test suggest that the spring coils clash in normal intended operation.

- The springs are mounted horizontally underneath the vehicle, but are unlikely to slip as there is a minimum spring height of 4.0 inches, corresponding to a load of 977 lbs (according to NAI Specification, Section 4.2.1.2 of NS-65-99), applied to the spring.

- As the spring was compressed, the coils were allowed to contact each other in service. This caused wear of the painted surface and exposed the metal beneath to the environment.

- It was stated in the supplied information and analyses from VRTC that the spring brake chambers were not sealed to the outside elements. Debris found in the chambers after they had been disassembled were made up of road dust, dirt, road cleaning salts, and sand that would be found on a typical construction site. This debris would have acted as abrasive media. Once they enter the chamber, or coat the surface of the spring, they can cause accelerated abrasion of the painted spring surface as it is compressed and the coils contact each other or the spring supports. This would serve to accelerate the

wear rate of the paint on the coil surface beyond that caused by coil-coil contact ("clashing") alone, exposing the metal beneath as observed.

- An additional consequence of the chamber being open to the atmosphere was that moisture from the air was allowed into the chamber. This moisture, together with any other potentially corrosive debris (e.g., salt) reacted with the exposed metal caused by the wearing away of the protective paint. This caused the accelerated oxidation and pitting observed on the metal surface.

- The supplied specification for paint application (ESF-3029-F) in *Environmental Requirements*, "B: Acceptance Requirements", Point1 states:

  > "…bare metal caused by contact between spring coils or between the spring and housing or spring and piston is not considered a defect."

  Bare metal caused by any of these factors is most definitely a defect. The paint's sole function is to prevent exposure of the steel to the environment. As has been observed in this study, the corrosion of the steel that has been exposed to the environment is a catalyst for the failure of all of the springs. It is recommend that a mechanical design that avoids coil clash or a coil coating system that can withstand the abrasion of clashing and secondary grinding media be applied to the spring surface in place of the paint currently used.

MICROSTRUCTURAL ANALYSIS

NAI Specification NS-65-99, Section 3.8.1, specifies that the microstructure of the spring material:

> "… shall exhibit a fine homogeneous tempered martensitic structure free from ferrite, intermediate transformation products, and/or detrimental inclusions."

Figure 4 shows the microstructures of Sample 78023-3 (4% nital etch), at regions close to the edge of the spring, and in it's core. Both regions are consistent with the specified microstructure.

HARDNESS TESTING

NAI Specification NS-65-99, Section 3.4.1, specifies that, "the spring shall be heat treated in order to obtain the specified hardness requirement listed on the drawing." The Haldex spring drawing supplied (for Part #3065001) stated that the hardness requirement is 50 to 53 HRC (Rockwell C scale).

NAI Specification NS-65-99, Section 3.6, calls for shot peening of the spring surface prior to painting. This process involves impacting the surface of the spring with steel shot to plastically deform the local surface layer, introducing compressive residual stresses at the surface. This practice is used to increase fatigue resistance of the component. It also causes a local hardening of the material at the surface, which would be detectable by performing a microhardness traverse from the bulk of the sample to the edge.

Macrohardness testing was performed on a cross-section of each spring. Macrohardness was taken in the core regions of sections cut from the spring samples and ground to have parallel edges. It was found that all springs conformed to the 50 to 53 HRC limit.

Next, a microhardness traverse was performed to determine the depth and hardness of the shot peened layer. Figure 5 shows the detail of the traverse. The hardness was measured at regular intervals from the core of the spring section to the edge. Figures 6 and 7 show the results of the traverses for Samples 78023-2 and 78063-2, respectively. With the exception of three likely erroneous data points for Sample 78023-2, both samples had a hardness that varied within the specified 50 to 53 HRC limits. No evidence of local surface hardening was found. It is apparent that shot peening has not been performed, or the material has been subsequently altered to remove the peened layer. The lack of this compressive stress surface layer means that the spring would have a lower resistance to fatigue crack initiation compared to a properly shot peened surface.

In addition to the hardness results, no surface deformation is visible in the microstructure. Peening would cause local deformation which would be visible in polished and etched metallurgical samples. This apparent lack of shot peening pushes the springs out of specification, as stated in NAI NS-65-99, Section 3.6.

MATERIALS CHEMISTRY

Table 1 shows the results of optical emission spectroscopy examination for each of the spring samples sent. The specified compositional limits under NAI NS-65-99 are also included in the table for comparison.

It was found that all spring samples met the compositional requirements laid out in the specification. The presence of copper (Cu), molybdenum (Mo), and vanadium (V) was suggested by the optical emission spectroscopy analysis. However, the quantity detected was close to or at the minimum resolution of the technique. The results do not constitute an out-of-specification result.

DECARBURIZATION

NAI Specification NS-65-99, Section 3.7.1, calls out limits for decarburization that may be caused by the heat treating process. Decarburization is the diffusion of carbon away from the surface regions of the coils due to oxidation with the furnace atmosphere during heat treatment (as specified in Section 3.4). The local removal of carbon from the surface of the coil produces a surface layer which is softer than the bulk material. The carbon serves to act as an interstitial hardener in the steel lattice. When it is removed, the lattice strains are reduced, thus causing softening of the material in this layer.

The spec states that the depth of partial surface decarburization shall not exceed 0.023 mm (23 µm). Each spring sample sent was tested by examining the microstructure at the 12, 3, 6, and 9 o'clock positions around the outer diameter (OD) of the sample. The 12 o'clock position was defined as the region of the spring's OD where the most paint was missing.

Figures 8 through 11 show the results of the examinations. Each image was taken at 100x magnification, and the scale bar is shown in the center of each figure. The limit of 23 µm is shown in a separate scale for easy comparison. The decarburized layer shows up on in the micrographs as a white layer at the paint/metal interface.

Overall, very little decarburization was observed in any sample, and none of what was observed exceeded the specified limit.

COATING THICKNESS

The coating thickness data provided by the VRTC indicated average thicknesses for the coating for each spring sample. The test was conducted only on regions where the paint was present on the spring OD. In regions of the circumference where there is no paint due to abrasion, it was impossible to tell if the coating thickness was in specification or not. Thus, the results are somewhat biased/skewed by this preferential sampling method. If the sampling was performed on predetermined regions of the spring OD, then the average thickness would be lower than reported, as the sample regions would include regions where there was a 0 mm paint thickness.

Further research into the exact application procedure of the paint (not reported) should be performed in order to improve the bonding to avoid exposure of the spring steel to the environment. Alternate corrosion protection coatings or a more corrosion resistant alloy should also be considered.

FRACTOGRAPHY/OPTICAL MICROSCOPY

Figures 12 through 16 show optical micrographs of the fracture surface of a selection of the failed springs provided. Samples 78023 B, 76369 A, and 78063 A were selected for analysis, as they represented the range of fracture surfaces sent. They were also the best preserved fracture surfaces sent (i.e., lowest quantity of surface oxidation, enabling surface features to be discerned more readily).

Figure 12 shows an as-received image of the fracture surface of Sample 78023 B. The reddish surface is caused by oxidation. Despite surface oxidation, it is clear that this fracture is a classic torsional fatigue failure. The beach marks on the surface clearly point back to a point of origin at the spring OD, as noted on in the figure. The fracture surface is helical in shape, consistent with a torsional failure mode. The origin appears to be a pit at the spring OD surface in a region where there is no paint adhered. Figure 13 is a composite image showing the distribution of paint on the OD surface. It is clear from this figure that where there is a lack of paint, the exposed metal surface is pitted and oxidized.

Figure 14 shows an as-received image of the fracture surface of Sample 76369 A. Again, this is a classic torsional fatigue failure. The origin again is a pit at the spring OD surface in a region

where the paint is not present. Figure 15 shows an image of the same fracture surface with the oxidation partially removed after application of dilute phosphoric acid solution. The fracture surface features are more clearly visible. The origin is definitely a pit at the OD surface.

Figure 16 shows the as-received fracture surface of Sample 78063 A. This again appears to be a torsional fatigue fracture surface. However, in this case the region that the beach marks point to as the origin is broken off from the sample. This is likely due to a secondary damage event that could have occurred either while the spring was still in service or on the VRTC test stand, but after it had already fractured. This spring also shows secondary cracking running in a helical pattern characteristic of torsional failures. This could have been due to the secondary loading imposed on the spring when in the VRTC test stand, rather than in service (the sample went through in excess of 2,000 cycles in the test stand before final failure). The figure shows clear abrasion marks on the surface of the paint adjacent to areas where the paint is no longer adhered to the spring.

The fracture surfaces indicate that in the regions where the paint has been removed (likely due to abrasion with debris and/or clashing of the coils) the surface of the metal was subject to pitting corrosion when exposed to the environment (e.g., salt and water). The pits act as stress concentrators, and are the initiation points for the final failure of the spring – a torsional fatigue failure. The fatigue crack grows as a result of the repeated cyclic loading of the spring. The spring is loaded in torsion, hence the observed fatigue failure mode.

It is likely that when the corrosion of the exposed metal begins, the corrosion spreads along the metal surface, and underneath the painted layer. Once this occurs the paint is no longer able to adhere to the metal surface, and is more easily removed in sections due to abrasion. This exposes more metal and the corrosion spreads.

SCANNING ELECTRON MICROSCOPY (SEM)

Figure 17 shows a summary of the SEM high magnification images taken of the fatigue fracture origin of Sample 78023 B. These images clearly show that the fracture initiated at a pit in the sample surface. Images (b) and (c) show a view of the corner of the fracture surface and the spring OD. The extent of the pitting corrosion present is very evident.

CONCLUSIONS

- The power springs failed due to torsional fatigue initiated at a corrosion pit on the spring OD caused by corrosion of the exposed steel in the environment in regions where the paint had de-bonded from the spring surface. Mechanical abrasion (by coil clashing and with secondary debris particles) led to removal of the paint, exposing the bare metal to the environment, inducing pitting corrosion, which in turn spread along the metal surface under the paint, causing yet more paint to become removed from the metal surface. The pits acted as stress concentrators and initiation points for a torsional fatigue final failure.

- Abrasion of the paint by clashing of spring coils was accelerated through interaction with debris causing it to de-bond in sections from the surface of the spring. The upper and lower spring coil also rubbed against the spring supports as the spring compressed.

- It is evident from the spring compression test on the intact spring that the spring coils do indeed clash (make mechanical contact) during normal intended operation of the spring. The contact occurs both between the points of contact with the housing end wall and pressure plate of the brake chamber, in addition to the coils of the spring contacting one another (clashing). It is recommended that the design be changed so as to avoid clashing between the spring coils and their support points during normal operation. Additionally, a coating system that is more wear resistant should be utilized to minimize loss of the corrosion protection barrier to the steel.

- The OD metal surface of the spring lacked the specified hardened compressive residual stress; a stress layer that should have been provided by the shot peening operation. This lowered its resistance to fatigue crack initiation. The presence of this layer alone would likely not have prevented the failure, but would have allowed the spring to be in service for a longer duration before a fatigue crack initiated. Nevertheless, the lack of this shot peened layer pushes the spring out of specification under NAI NS-65-99, Section 3.6.

- Materials chemistry and microstructure appear to be within specified limits.

- The acceptance criteria in ESF-3029-F were flawed in that they allowed exposed metal caused by coil clashing or contact with spring supports to pass inspection. It is recommended that these criteria be changed to only allow springs to pass with a complete coating of paint remaining after testing. Again, the mechanical design should

be changed to avoid coil clashing, or at the very least specify a more durable protective coating.

- Further research into the exact application procedure of the paint (not reported) should be performed in order to improve the bonding to avoid exposure of the spring steel to the environment. Alternate corrosion protection coatings or a more corrosion resistant alloy should also be considered.

Table 1

CHEMICAL COMPOSITION OF SPRING SAMPLES BY OPTICAL EMISSION SPECTROSCOPY

Element (wt. %)	NS-65-99 Spec.	LS1	76039	76369	78023	78063
Carbon (C)	0.50 – 0.61	0.55	0.55	0.53	0.58	0.56
Chromium (Cr)	0.50 – 0.80	0.69	0.68	0.67	0.73	0.69
Copper (Cu)	N/A	0.01	0.01	0.01	0.01	<0.005
Manganese (Mn)	0.50 – 0.80	0.72	0.71	0.70	0.75	0.72
Molybdenum (Mo)	N/A	0.01	<0.005	<0.005	<0.005	<0.005
Nickel (Ni)	0.25 max.	0.02	0.02	0.02	0.01	0.02
Phosphorus (P)	0.04 max.	0.012	0.013	0.011	0.010	0.011
Silicon (Si)	1.20 – 1.60	1.33	1.30	1.32	1.46	1.37
Sulfur (S)	0.04 max.	<0.005	0.007	0.005	0.006	<0.005
Vanadium (V)	N/A	<0.005	<0.005	<0.005	<0.005	<0.005

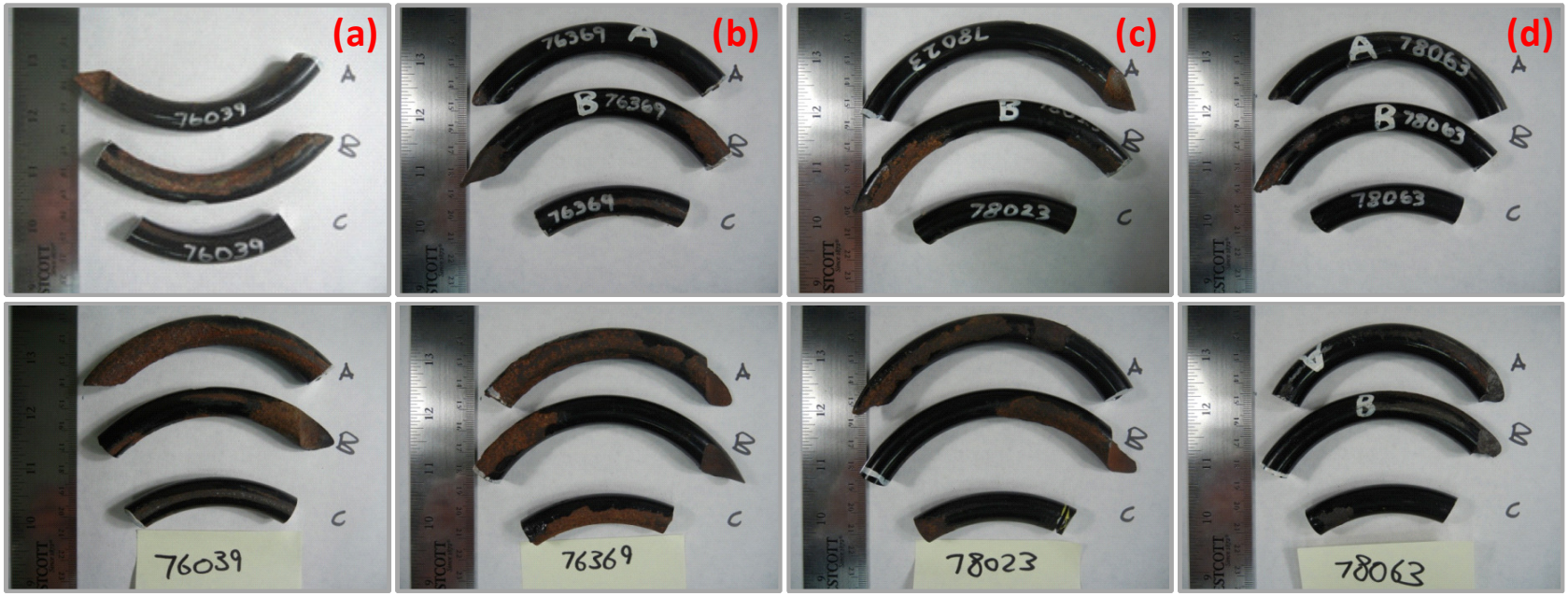


Figure 1 – Photos of the As-received Broken Spring Sections.

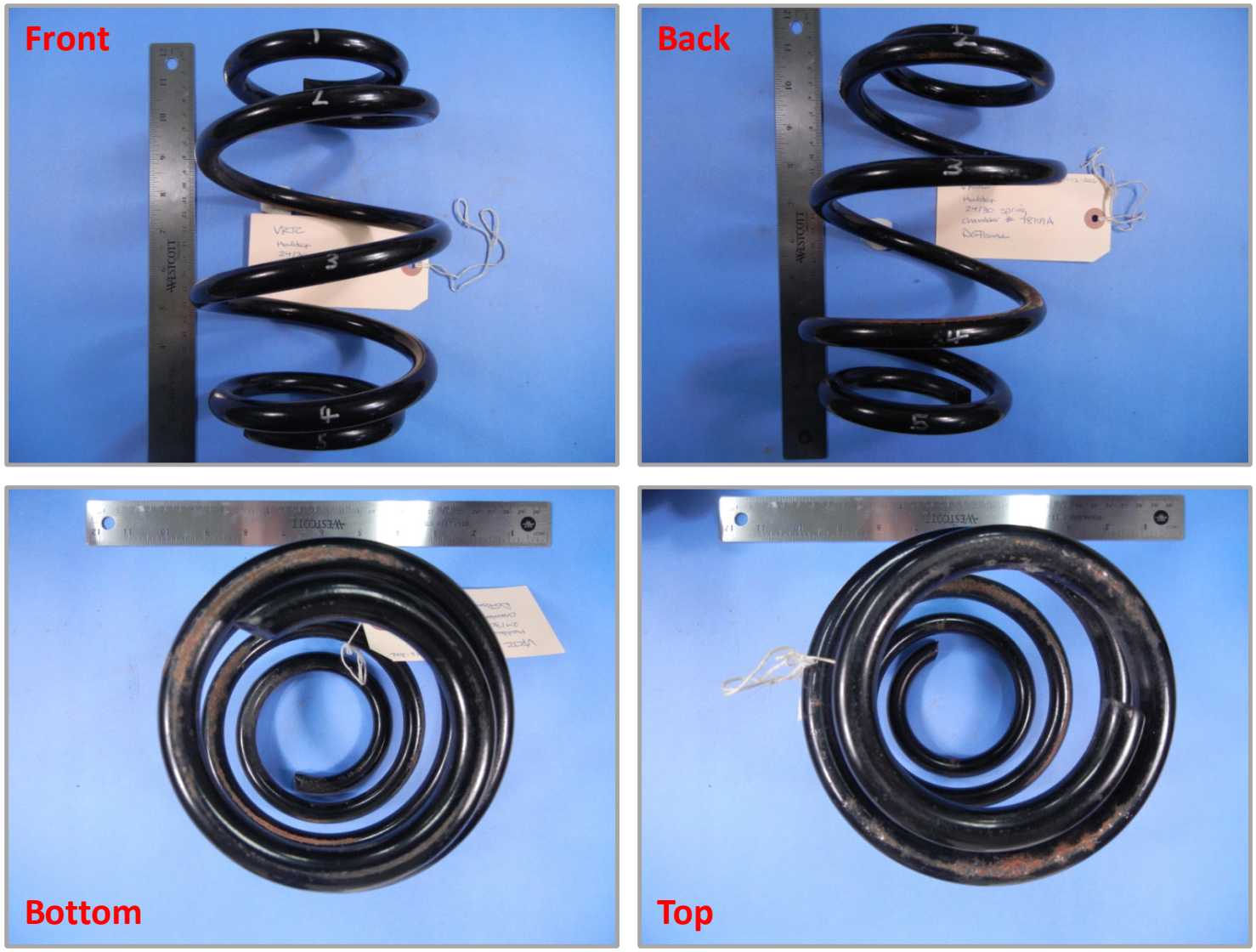


Figure 2(a) — Photos of the As-received Intact, Used Spring.



Figure 2 (b) — As-received Intact, Used Spring. Close-up Images of the Wear Regions.

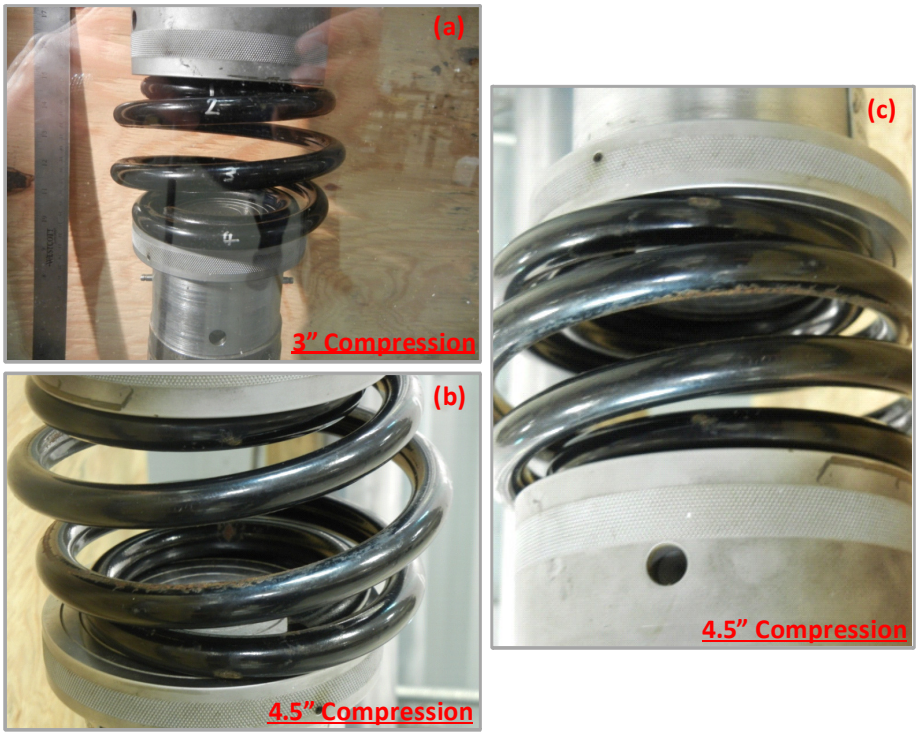


Figure 3 — Compression Test of Intact Spring, Showing How Coils Interact Upon Compression.

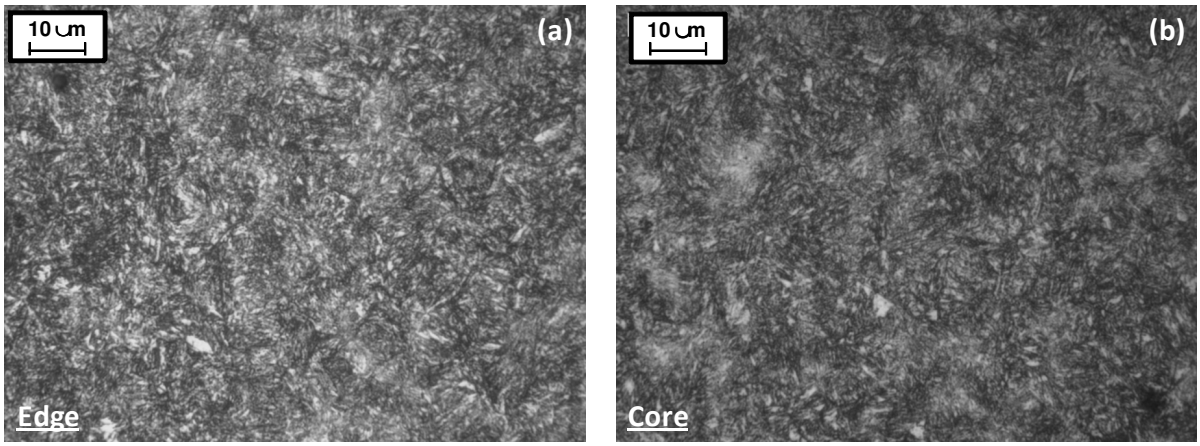


Figure 4 — Microstructure – Sample 78023-3 (Nital Etch). Quenched and Tempered Martensite Structure.

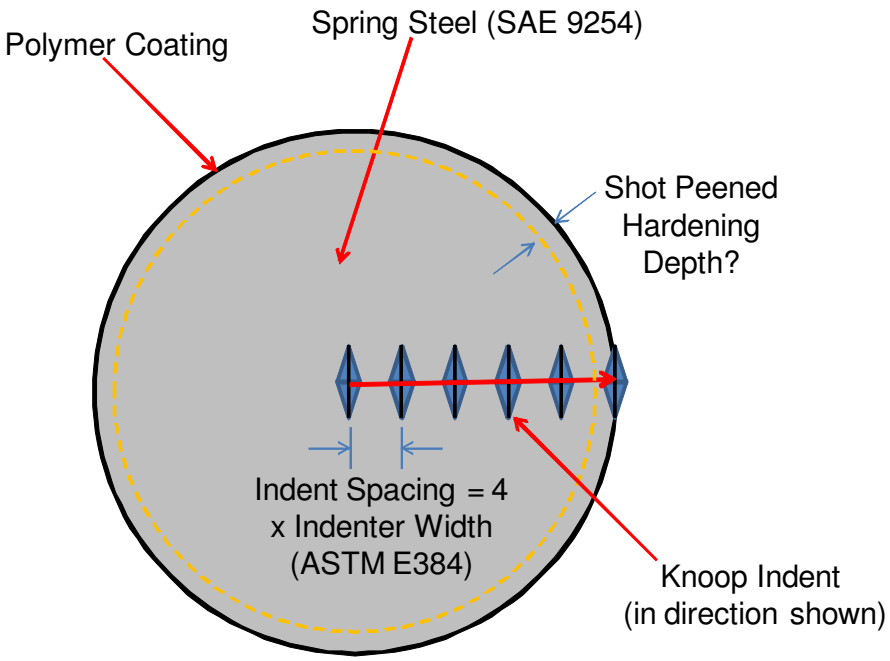


Figure 5 — Details of Microhardness Traverse.

Distance from Core (")	Hardness (HK500)	Hardness (HRC) - Calculated
0.01	520.6	48.6
0.02	563.1	51.2
0.03	564.1	51.3
0.04	565.1	51.3
0.05	593.4	52.9
0.06	558.2	51
0.07	560.1	51.1
0.08	578.5	52.1
0.09	580.6	52.2
0.1	522.4	48.7
0.11	570.2	51.6
0.12	558.2	51
0.13	571.2	51.7
0.14	572.3	51.7
0.15	580.6	52.2
0.16	593.4	52.9
0.17	588	52.6
0.18	582.7	52.3
0.19	585.8	52.5
0.2	589	52.7
0.21	593.4	52.9
0.22	583.7	52.4
0.23	574.3	51.9
0.24	588	52.6
0.25	586.9	52.6
0.258	530.6	49.2

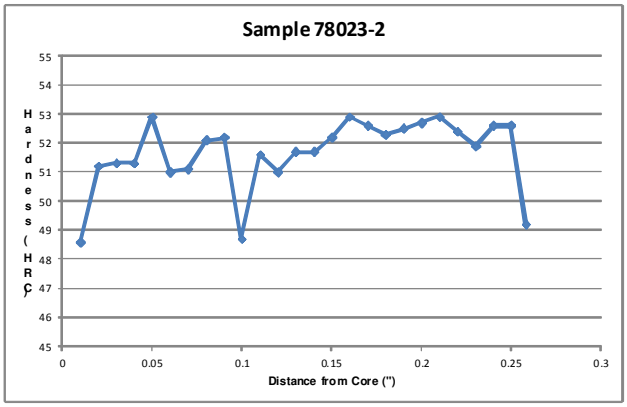


Figure 6 — Results of the Microhardness Traverse for Sample 78023-2.

Distance from Core (")	Hardness (HK500)	Hardness (HRC) - Calculated
0.01	556.2	50.8
0.02	549.4	50.4
0.03	561.1	51.1
0.04	572.3	51.7
0.05	556.2	50.8
0.06	575.4	51.9
0.07	576.4	52
0.08	559.1	51
0.09	567.2	51.5
0.1	583.7	52.4
0.11	574.3	51.9
0.12	576.4	52
0.13	583.7	52.4
0.14	575.4	51.9
0.15	584.8	52.4
0.16	570.2	51.6
0.17	580.6	52.2
0.18	578.5	52.1
0.19	580.6	52.2
0.2	574.3	51.9
0.21	575.4	51.9
0.22	586.9	52.6
0.23	571.2	51.7
0.24	575.4	51.9
0.25	594.4	53
0.256	570.2	51.6

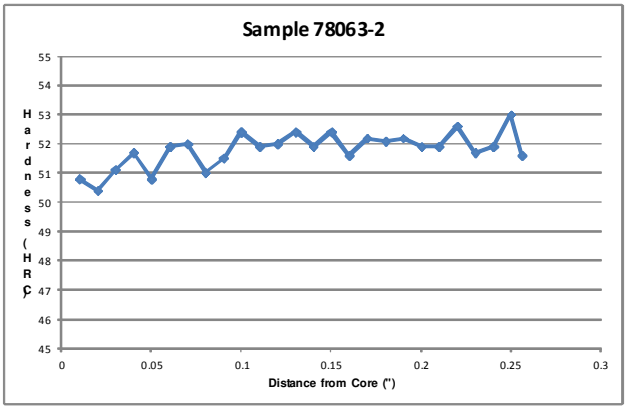


Figure 7 — Results of the Microhardness Traverse for Sample 78063-2.

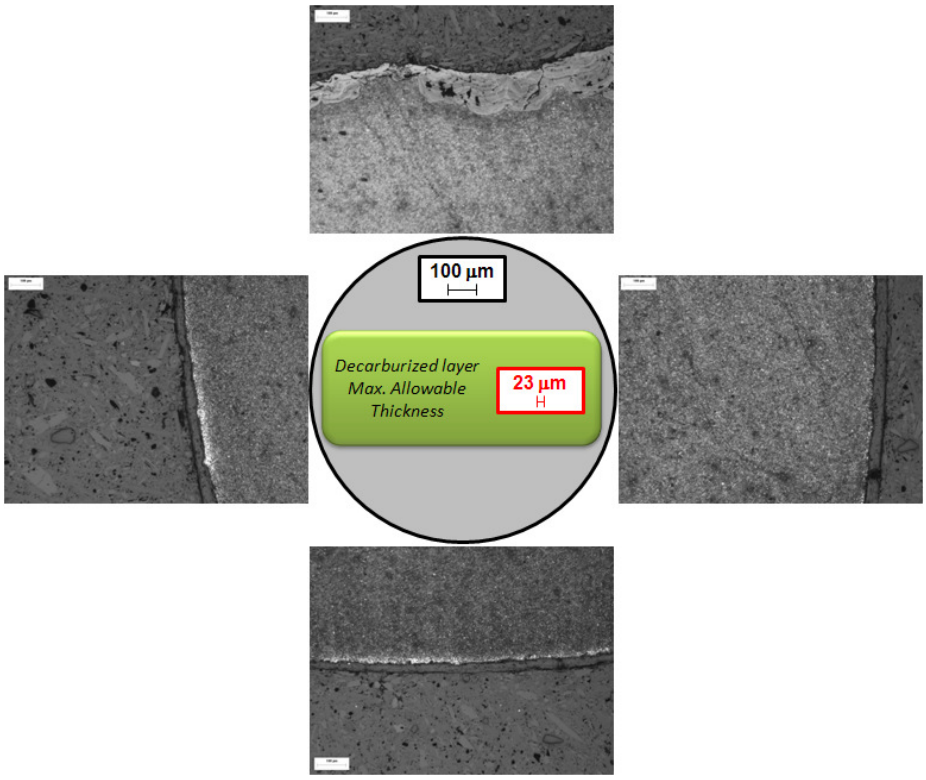


Figure 8 — Decarburization Study Results for Sample 78023.

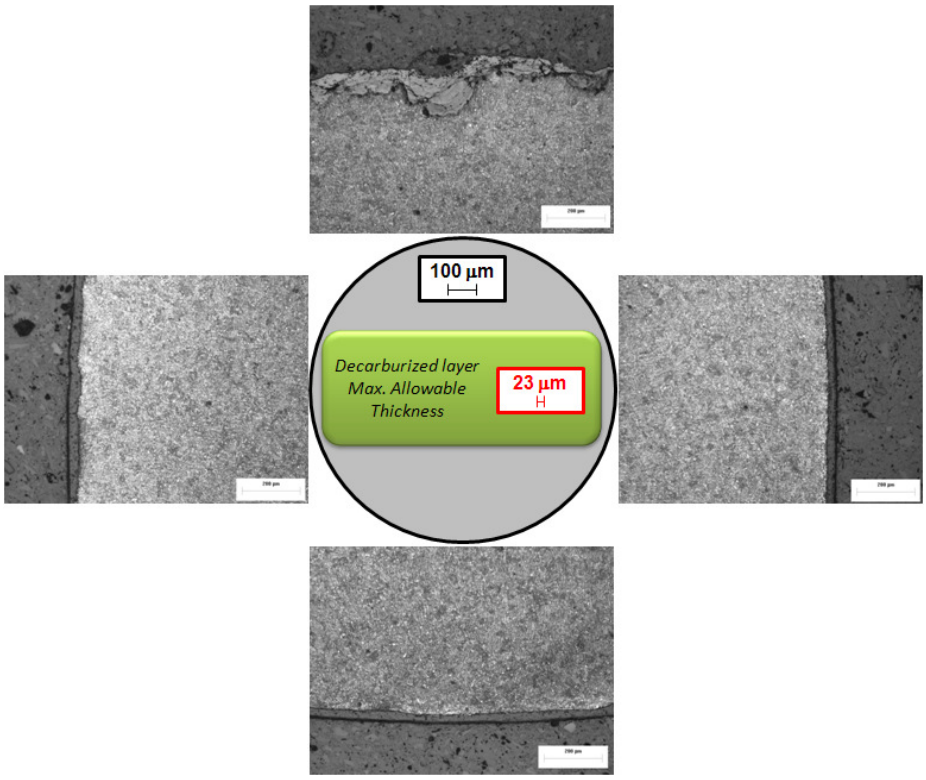


Figure 9 – Decarburization Study Results for Sample 76039.

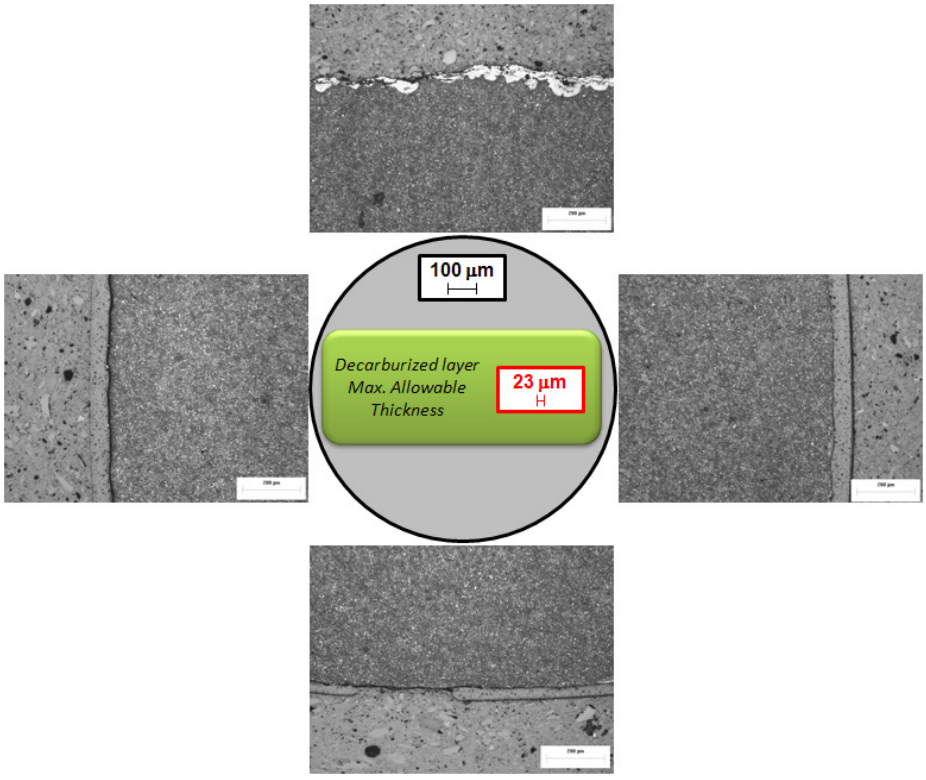


Figure 10 — Decarburization Study Results for Sample 78063.

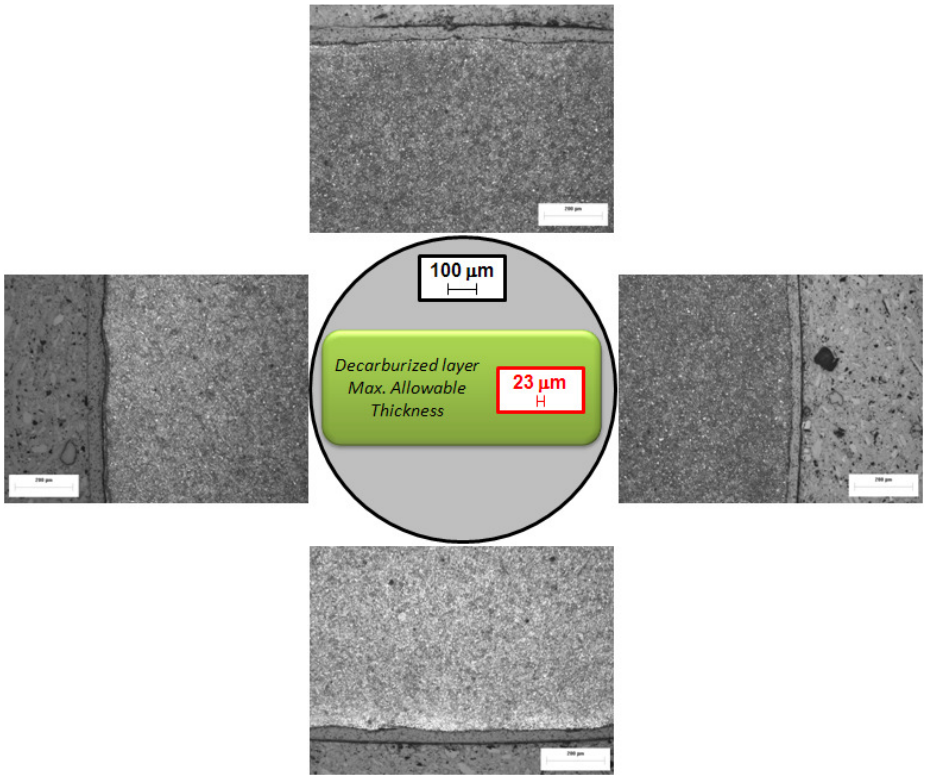


Figure 11 — Decarburization Study Results for Sample LS1.

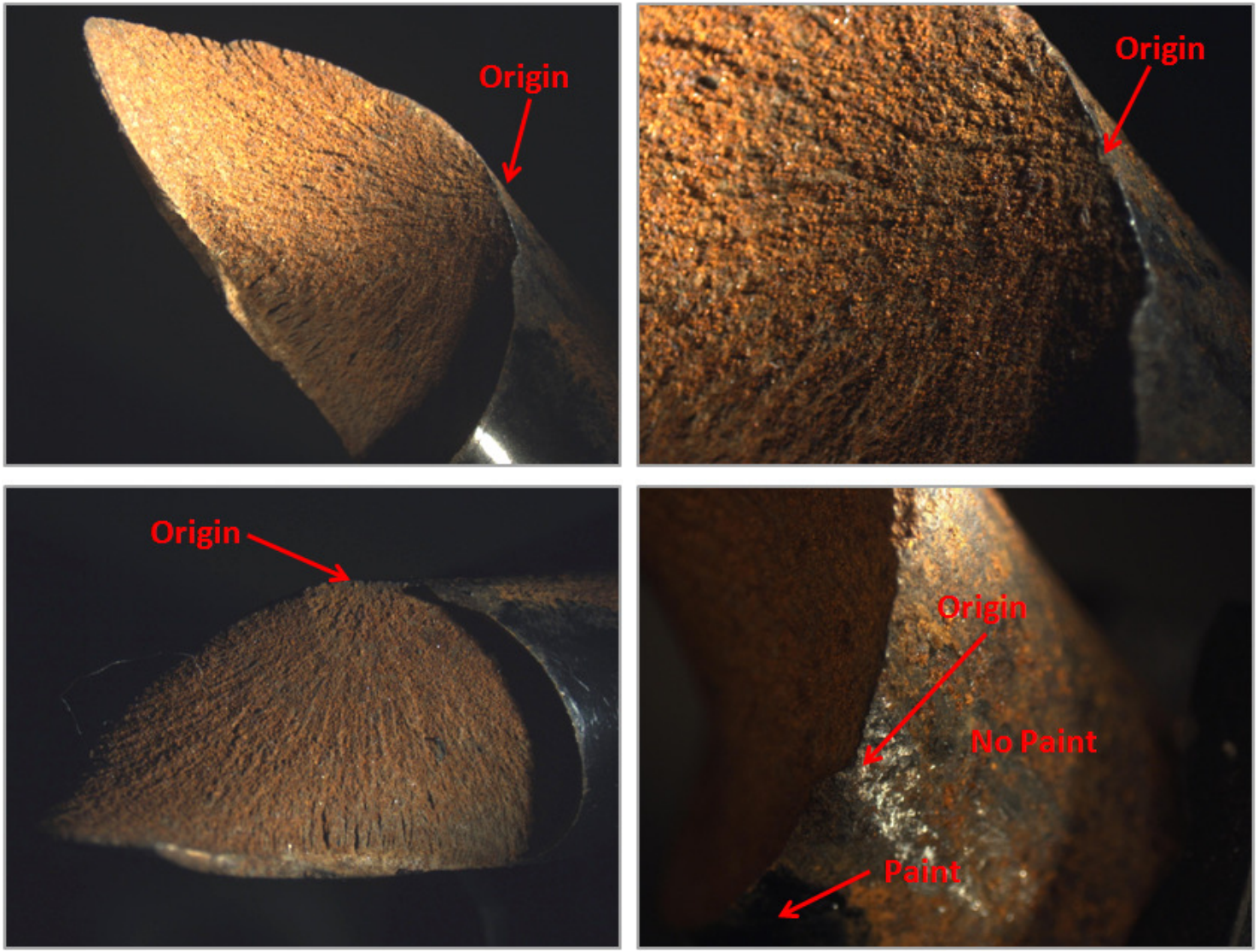


Figure 12 — Optical Micrographs of the Fracture Surface of Sample 78023 B.

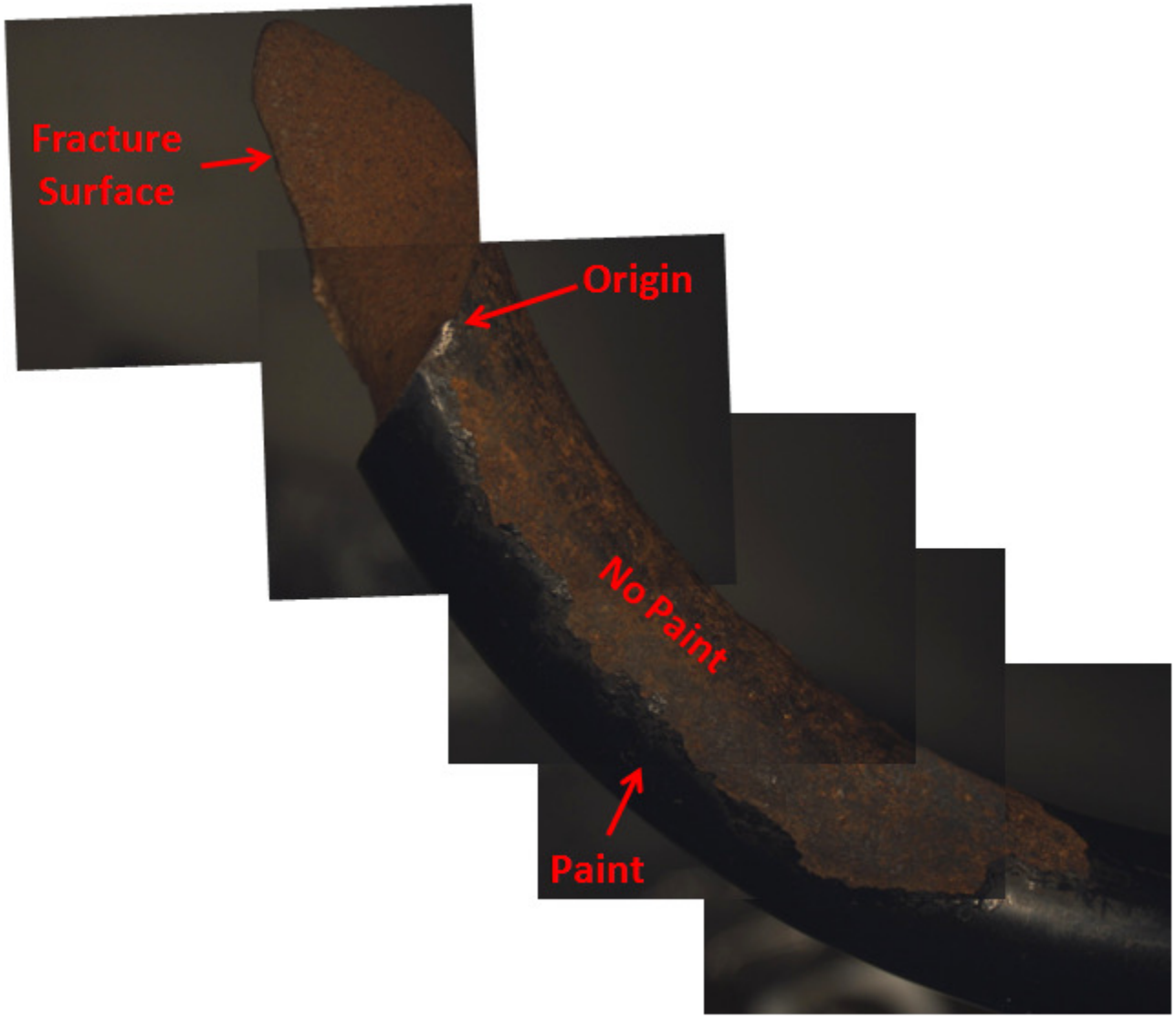


Figure 13 — Composite Optical Micrograph Image Showing Spring OD Surface of Sample 78023 B Local to the Fracture.

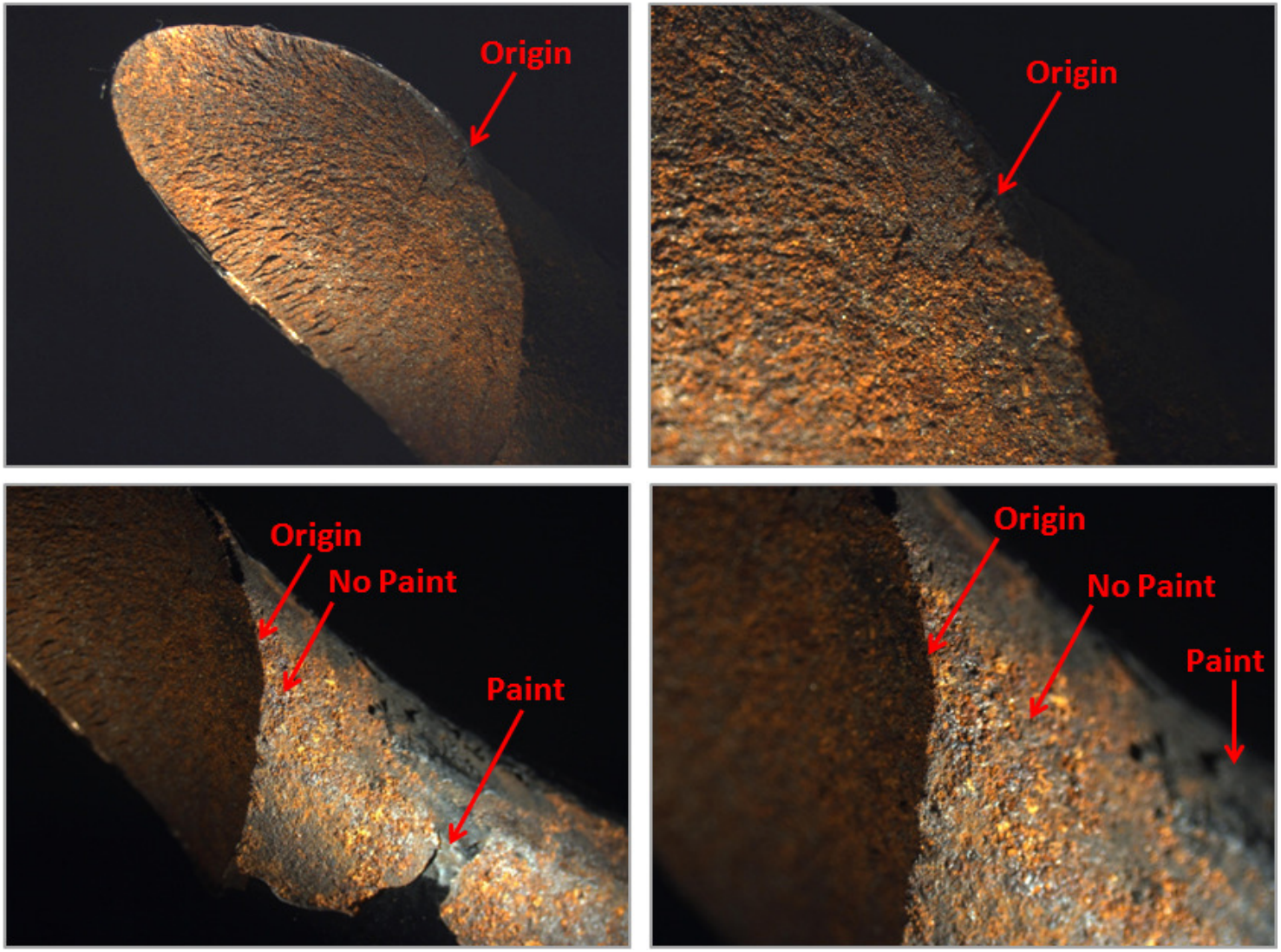


Figure 14 — Optical Micrographs of the Fracture Surface of Sample 76369 A.

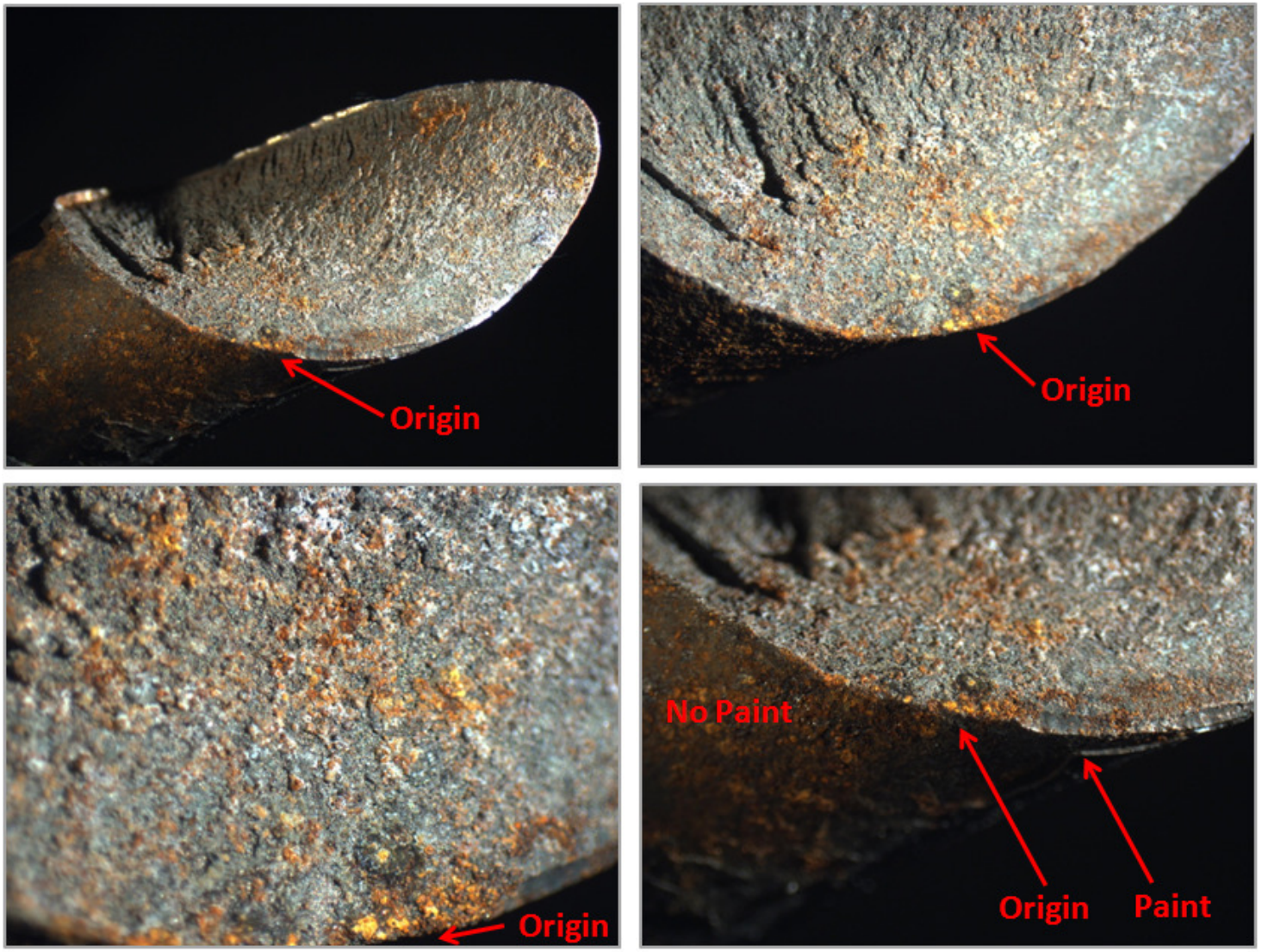


Figure 15 — Optical Micrographs of Fracture Surface of Sample 76369 A, Cleaned with Dilute Phosphoric Acid Solution.

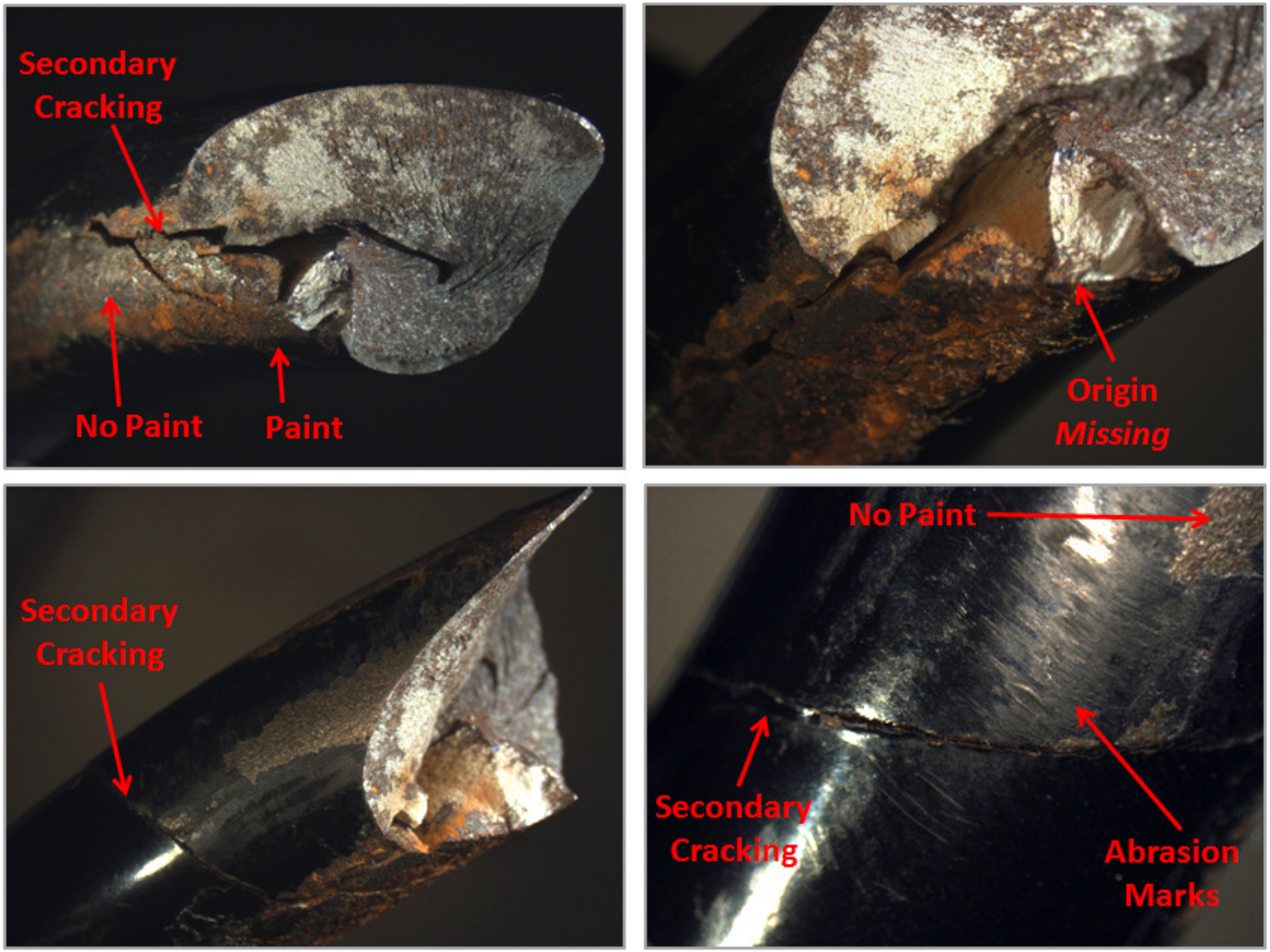


Figure 16 — Optical Micrographs of the Fracture Surface of Sample 78063 A.

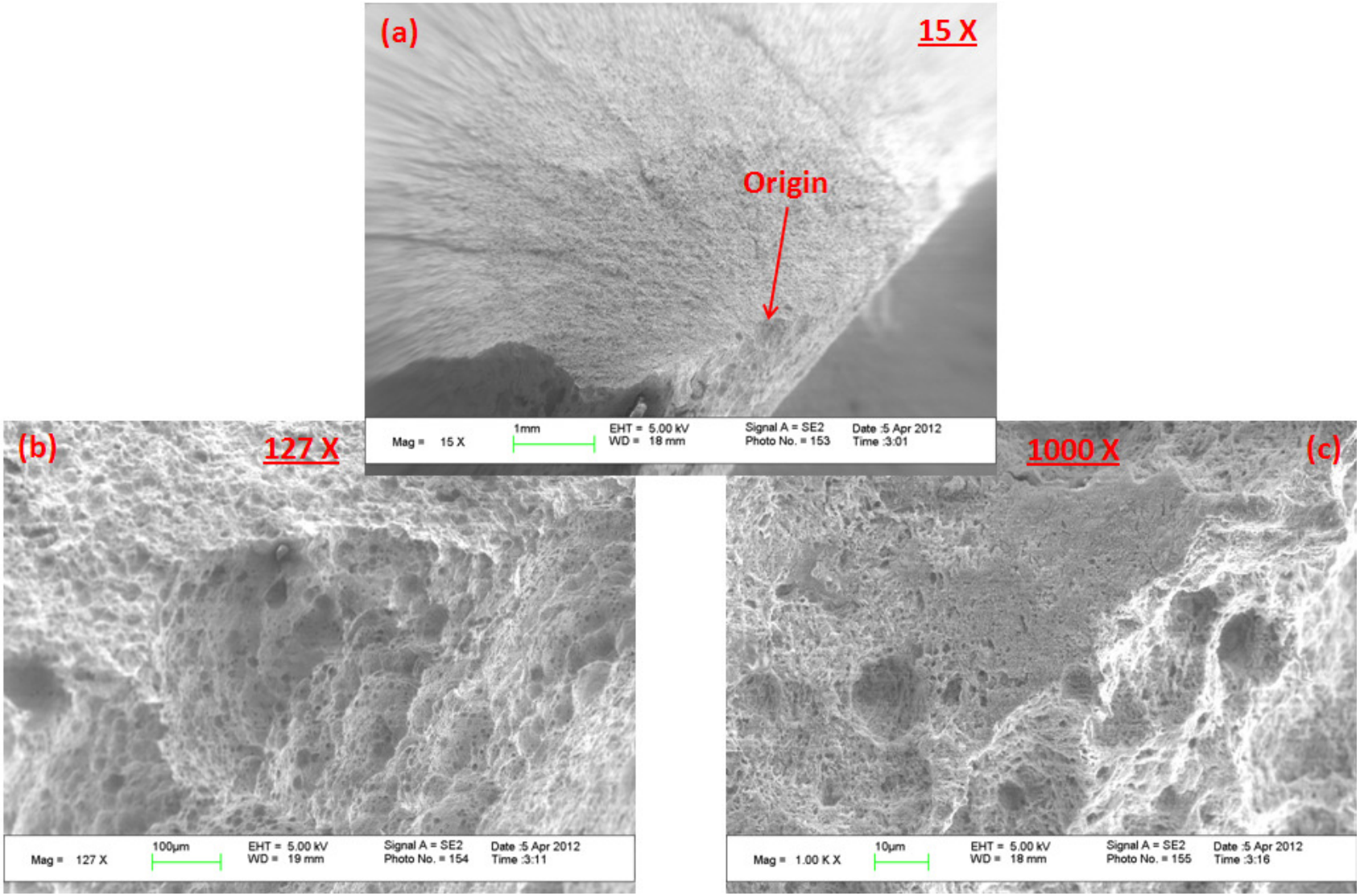


Figure 17 – SEM Images of the Fracture Surface Origin of Sample 78023 B.